



# Solvent-free, one-pot mechanochemical synthesis of high-DS cellulose esters with tunable thermoplasticity

Zhongkai Xu<sup>a,b</sup>, Fangyue Cheng<sup>b</sup>, Qingbo Zhao<sup>b</sup>, Zhenxing Wu<sup>b</sup>, Peng Wei<sup>c,\*</sup>,  
Chunzu Cheng<sup>b,\*</sup>, Shi-Zhong Luo<sup>a,\*</sup>

<sup>a</sup> State Key Laboratory of Green Biomanufacturing, College of Life Science and Technology, Beijing University of Chemical Technology, Beijing, 100029, China

<sup>b</sup> State Key Laboratory of Bio-based Fiber Materials, China Textile Academy, Beijing, 100025, China

<sup>c</sup> School of Traditional Chinese Medicine, Beijing University of Chinese Medicine, Beijing, 102488, China

## ARTICLE INFO

### Keywords:

Acyl chloride  
Cellulose  
Cellulose ester  
Esterification reaction  
Mechanochemical reaction

## ABSTRACT

Cellulose esters represent promising thermoplastic biobased materials. However, their conventional synthesis often relies on the use of ionic liquids or substantial quantities of pyridine and acid anhydrides. This study presents an alternative approach in which cellulose was first converted to alkali cellulose using sodium hydroxide solution, followed by a mechanochemical reaction with acyl chlorides to obtain thermoplastic cellulose esters with a degree of substitution (DS) above 2.5. Hydrolysis of the acyl chloride was effectively suppressed by using conjugated and hydrophobic benzene-ring structures along with low reaction temperatures, which promoted efficient grafting onto cellulose even in the presence of water. The resulting para-substituted benzoyl cellulose esters exhibit clear thermoplasticity, with a measurable glass-transition temperature (T<sub>g</sub>) and a thermal decomposition temperature approximately 30 °C higher than that of native cellulose. By varying the alkyl chain length attached to the rigid benzene ring, both T<sub>g</sub> (from 175 °C for methyl to 151 °C for heptyl) and mechanical properties (strength and elongation) could be tuned. Moreover, external plasticization with triethyl citrate further lowered the T<sub>g</sub> to 98 °C, significantly improving the melt-processability. This solvent- and catalyst-free mechanochemical method eliminates the need for pyridine or anhydrides, offering a scalable route to high-performance cellulose-based thermoplastics.

## 1. Introduction

The increasing consumption of petroleum resources (Mori, 2023; Naser et al., 2021) has driven growing interest in cellulose (Li, Chen, et al., 2021; Pan et al., 2024; Qian et al., 2025; Song et al., 2018) as the most abundant natural polymer on Earth (Jiang et al., 2020; Sawatdee et al., 2025; Zhang et al., 2018). However, the inherent inability of cellulose to be melt-processed significantly restricts its range of applications (Bonifacio et al., 2023; Sessini et al., 2021; Wang et al., 2020). Chemical derivatization has therefore become a key strategy to enhance the processability of this renewable resource (Ahokas et al., 2025; Li et al., 2025; Li et al., 2022; Lu et al., 2025; Zhou et al., 2024). Notable early examples include viscose cellulose fiber, the first industrialized synthetic fiber (Mendes et al., 2021), and nitrocellulose (celluloid), the first historical plastic material (Bussiere et al., 2014). More recently, researchers have focused on derivatizing cellulose to impart melt-processability and other desirable properties, such as recyclability in

aqueous systems (Wang et al., 2025; Yin et al., 2024; Yin et al., 2026) and biodegradability (Hirose et al., 2019; Li, Qiu, et al., 2024).

From a processing standpoint, cellulose derivatization routes fall into two broad categories: homogeneous (Pei et al., 2020; Tanaka et al., 2017; Yun et al., 2025) and heterogeneous reactions (Huang et al., 2012; Lease et al., 2021; Shojaeiarani et al., 2018; Xia et al., 2023). Homogeneous reactions offer an ideal platform for investigating the structure-property relationships of cellulose derivatives (Chen et al., 2018; Tanaka et al., 2017; Xu et al., 2024). This approach typically requires complete dissolution of cellulose in an ionic liquid to form a molecularly homogeneous solution, enabling quantitative reactant feeding and precise process control (Li, Qiu, et al., 2024; Tanaka et al., 2017; Yin et al., 2024). However, the initial dissolution step itself constitutes a form of cellulose processing, rendering subsequent steps—such as reaction, precipitation, or melt-processing—technologically redundant. Moreover, on an industrial scale, dissolution processes based on ionic liquids face both technical and economic challenges. Therefore, while homogeneous

\* Corresponding authors.

E-mail addresses: [weipeng@bucm.edu.cn](mailto:weipeng@bucm.edu.cn) (P. Wei), [chengchunzu@cta.gt.cn](mailto:chengchunzu@cta.gt.cn) (C. Cheng), [luosz@mail.buct.edu.cn](mailto:luosz@mail.buct.edu.cn) (S.-Z. Luo).

<https://doi.org/10.1016/j.carbpol.2026.125258>

Received 3 January 2026; Received in revised form 25 March 2026; Accepted 27 March 2026

Available online 29 March 2026

0144-8617/© 2026 Elsevier Ltd. All rights reserved, including those for text and data mining, AI training, and similar technologies.

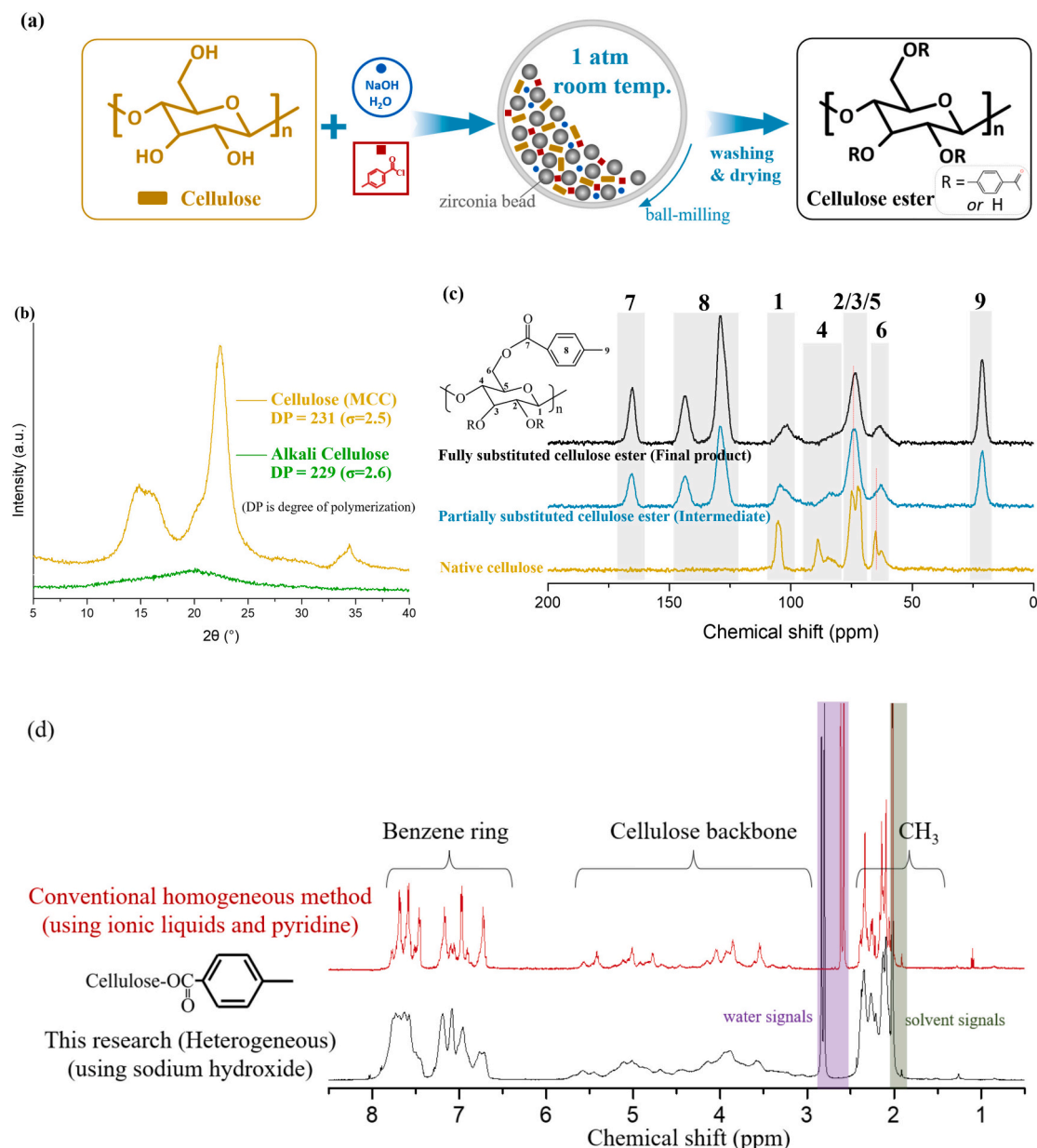


**Fig. 1.** Mechanochemical synthesis, structural evolution, and comparative analysis of cellulose esters: (a) Schematic illustration of the one-pot heterogeneous synthesis from alkali cellulose; (b) Evolution of cellulose crystallinity and degree of polymerization (DP) with ball-milling time. (c) <sup>13</sup>C NMR spectrum indicating the regiospecific acylation at C-6, followed by C-2/C-3; (d) Comparative <sup>1</sup>H NMR spectra of cellulose ester prepared via the present heterogeneous route (bottom) and a conventional homogeneous method (top) (in acetone-*d*<sub>6</sub>).

systems hold considerable value for fundamental research, their industrial implementation remains limited.

In contrast, heterogeneous reactions are widely regarded as promising for large-scale applications and have been successfully employed in the commercial production of materials such as cellulose acetate (CA) (Mphateng et al., 2025; Tanaka et al., 2016) and hydroxypropyl methylcellulose (HPMC) (Joshi et al., 2019a; Siepmann & Peppas, 2012). Nevertheless, they suffer from significant drawbacks, including difficulties in precise control over product structure (Hou, Yuan, et al., 2023), poor reaction uniformity (Toyama et al., 2015; Yin et al., 2024), and generally low degrees of substitution (Hou et al., 2021; Zhu et al., 2021). To address these solid-liquid contact limitations, various intensification methods have been developed, including microwave (Nemr et al., 2016), ultrasound (Chatel & Varma, 2019), ball milling (Hou et al., 2024; Kuga & Wu, 2019), screw extrusion (Zhong et al., 2013), and other heterogeneous methodologies (Thiebaud & Borredon, 1995).

However, existing heterogeneous processes remain constrained in terms of the types of functional groups that can be introduced and the choice of reaction media. For instance, HPMC production relies on the reaction of alkali cellulose with small epoxy or halogenated reagents (with ≤ 4 carbon atoms) (Joshi et al., 2019b; Klemm et al., 1998). When acyl chlorides are used, a large excess of pyridine (> 6 mol per mol cellulose) is typically required as an acid scavenger in non-aqueous systems (Ge et al., 2022; Hou et al., 2024), which limits practical application due to its toxicity and high consumption. Previous work on acyl chloride/alkali cellulose systems typically yielded low DS values (< 1) (Kita et al., 1926; Kwatra et al., 1992; Li et al., 2011; Sundman et al., 2015) and remained at the level of mechanistic exploration (Fox et al., 2011), without leading to an application-oriented material platform. This limited success reflects the topochemical effects inherent to heterogeneous cellulose derivatization (Hou, Li, et al., 2023; Kostag et al., 2019), wherein non-uniform substitution patterns along the polymer chain are

intrinsically difficult to avoid. Achieving a high overall DS is a critical prerequisite for obtaining cellulose derivatives with consistent, uniform macroscopic properties from a heterogeneous process (Hou, Li, et al., 2023; Joshi et al., 2019b; Kostag et al., 2019). Similarly, the anhydride route-exemplified by cellulose acetate production-is restricted by difficulties in introducing bulky molecular groups (Li et al., 2020; Li, Hou, et al., 2024). Although the combination of trifluoroacetic anhydride and ball milling enables the direct or indirect synthesis of thermoplastic cellulose esters (Li, Hou, et al., 2024), the widespread use of trifluoroacetic anhydride impedes large-scale adoption.

Despite the industrial appeal of heterogeneous reactions, their widespread adoption is constrained by intrinsic limitations: low efficiency, reliance on toxic auxiliaries (e.g., pyridine), and narrow structural versatility. We hypothesize that these limitations can be simultaneously overcome by a mechanochemical strategy employing conjugated, hydrophobic acyl chlorides (e.g., benzoyl chlorides) in the presence of water. This hypothesis is distinct from prior approaches: it posits that the molecular design of the reagent itself (conjugation reducing electrophilicity, aromatic rings imparting hydrophobicity) can inherently suppress hydrolysis in aqueous-alkaline media, rather than relying on water-free conditions or stoichiometric acid scavengers. Coupled with ball-milling to activate cellulose and ensure efficient contact, this approach should enable the direct synthesis of high-DS cellulose esters without pyridine or anhydrides. Proving this hypothesis correct is significant because it would establish a truly scalable heterogeneous pathway to thermoplastic cellulose esters, bridging the gap between the precise control of homogeneous systems and the practical requirements of industrial manufacturing.

## 2. Experimental

### 2.1. Materials

Microcrystalline cellulose (MCC, DP = 200, 200 mesh) were supplied by Aladdin Ltd. (China) (Microcrystalline cellulose was dried at 105 °C for 30 min prior to use). Laboratory sodium hydroxide, sodium carbonate, potassium hydroxide and ethanol were used throughout. All the acyl chlorides used in this study were purchased from Aladdin Ltd. (China). All reagents were of analytical grade and used without further purification.

### 2.2. Synthesis

Cellulose esters were synthesized according to Fig. 1. A typical procedure is given below. In brief, 0.33 g of dried MCC corresponding to 2 mmol of anhydroglucose units (AGU) and sodium hydroxide solution (1.5 ml, 40% (w/w)) were added into a 500 ml of zirconium mill pot filled with zirconium beads (50 balls with a diameter of 8 mm and 100 balls with a diameter of 4 mm), and the mill pot was transferred onto a planetary ball mill (QM-4 L, Nanjing Chishun Science & Technology Co., Ltd., China.) and milled for 0.5 h with rotational speeds of 400 rpm/min. Then 12 mmol acyl chloride reagent were added into the mill pot and milled for designated durations (0.5, 1, 2, and 4 h) designated temperatures (20, 50, and 80 °C) with appointed rotational speeds (100, 200, 300, 400, and 500 rpm/min). After the mechanochemical reaction, 80 mL of ethanol was added to the mill pot to dilute the obtained slurry, and milled for 15 min. Then, the sediment was collected and subjected to Soxhlet extraction with ethanol for 48 h. Subsequently, the product was washed three times with hot water (100 °C, 200 mL, filtration) under stirring to ensure complete removal of inorganic salts (e.g., NaCl, NaOH). Finally, the obtained products were dried in a vacuum oven at 60 °C for further characterization.

To enable a direct and fair comparison, a control sample of cellulose ester was prepared using a conventional homogeneous method in an ionic liquid (Chen et al., 2018; Yin et al., 2024; Yin et al., 2026), following well-established literature procedures (Section S1, Supporting

Information).

### 2.3. Characterization

#### 2.3.1. Nuclear magnetic resonance (NMR)

<sup>1</sup>H NMR and <sup>13</sup>C NMR spectra were recorded on a Bruker AV-400 spectrometer (400 MHz) at room temperature using acetone-*d*<sub>6</sub> or chloroform-*d* as solvent, with 16 scans or 5120 scans. DS values were also calculated from the integrated peak areas in the <sup>1</sup>H NMR spectra (Table S1-S6, Supporting Information). <sup>13</sup>C NMR spectra were acquired on a Bruker Avance-400 spectrometer (100 MHz) under cross-polarization conditions: spectral width 5000 Hz, contact time 2 ms, relaxation delay 6 s. HSQC-NMR spectra were recorded on a Bruker AV-600 spectrometer (600 MHz) at room temperature using acetone-*d*<sub>6</sub>.

#### 2.3.2. Degree of substitution (DS) by mass balance

(Mass DS values are provided for reference only; definitive DS values are determined by quantitative <sup>1</sup>H NMR spectroscopy). The DS was determined gravimetrically based on the mass change during esterification. The DS was calculated using Eq. 1:

$$DS \times (M - 35.5) + 162 - DS \times 17 = 162 \times m_2/m_1 \quad (1)$$

Where, *M* is the molecular weight of acyl chloride reagent, *m*<sub>1</sub> is the mass of initial cellulose, and *m*<sub>2</sub> is the mass of the resulting cellulose ester.

#### 2.3.3. Fourier transform infrared spectroscopy (FTIR)

Spectra were collected on a Jasco-6030 FT-IR spectrometer in the range 500–4000 cm<sup>−1</sup> with 16 scans.

#### 2.3.4. X-ray diffraction (XRD)

Patterns were obtained using a Siemens-Bruker D5000 diffractometer with Cu Kα radiation (λ = 1.5406 Å). Data were collected in the 2θ range of 5–45° with a step size of 0.05°.

#### 2.3.5. Thermal analysis

Differential scanning calorimetry (DSC) was performed on a PerkinElmer 4000 A instrument under N<sub>2</sub> flow (20 mL·min<sup>−1</sup>). Samples (10–20 mg) were heated from 25 to 400 °C at 20 °C·min<sup>−1</sup>. Thermogravimetric analysis (TGA) was carried out on a PerkinElmer TGA4000 under N<sub>2</sub> (30 mL·min<sup>−1</sup>), heating from 25 to 800 °C at 20 °C·min<sup>−1</sup>.

#### 2.3.6. Degree of polymerization (DP)

The DP of cellulose was determined according to GB/T 5881–2024 by measuring the viscosity of a copper ethylenediamine solution.

#### 2.3.7. Melt-flow observation

The thermal flow behavior was monitored using an Olympus BX51 polarized optical microscope equipped with a hot stage. Samples sandwiched between cover glasses were heated from 25 to 260 °C at 20 °C·min<sup>−1</sup>.

#### 2.3.8. Mechanical testing

Tensile properties were measured using an AGS-X-10kN universal testing machine (Shimadzu). Five replicates were tested for each sample, and the average values are reported.

#### 2.3.9. Scanning electron microscopy (SEM)

Morphological observations were performed on a Hitachi S-4700 SEM operated at 8–10 kV. Samples were sputter-coated with = 20 nm of copper prior to imaging to ensure conductivity.

#### 2.3.10. Dynamic mechanical analysis (DMA)

A Rheometrics Scientific DMA-850 analyzer was used in tension mode. Film specimens (length 6 mm, width 4 mm, thickness 0.1–0.3 mm) were tested at a fixed frequency of 1 Hz and a strain limit of 0.02%,

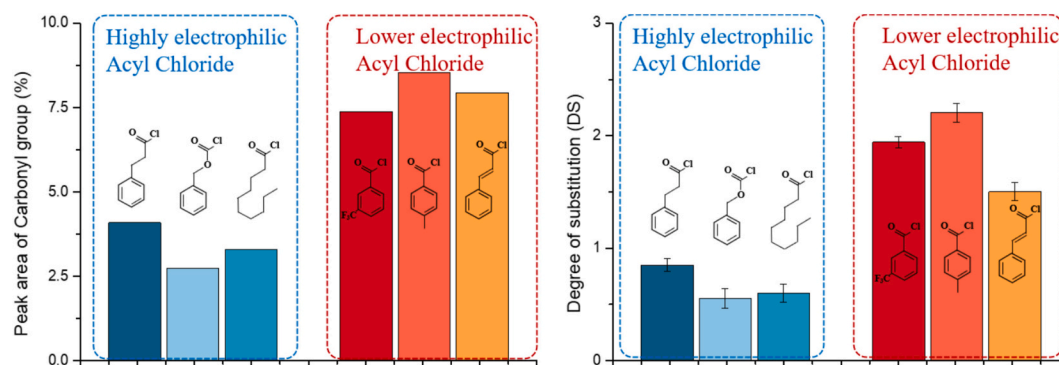


**Fig. 2.** Effect of acyl chloride electrophilicity on esterification efficiency. (a) Relative carbonyl absorption area in FT-IR spectra, used to estimate the degree of substitution (DS). (b) Experimentally determined DS values of cellulose esters prepared from acyl chlorides of different reactivities (The bar heights, derived from mass balance, are shown to illustrate the pronounced difference in reactivity; accurate DS values are determined by  $^1\text{H}$  NMR).

while heating from 25 °C at 2 °C·min<sup>-1</sup>.

### 2.3.11. Film preparation

Films were prepared by hot-pressing the dried cellulose ester powders between two aluminum foil sheets using a laboratory hot press. A typical procedure involved pre-heating the plates to 180 °C, applying a pressure of 5 MPa to the sample for 5 min, and then cooling the resulting film to room temperature.

### 2.3.12. Small-angle X-ray scattering (SAXS)

Measurements were conducted on a BL16B beamline (Donghua University) using an X-ray energy of 10 keV ( $\lambda = 0.135$  nm). The sample-to-detector distance was 140 mm, and exposure time was 100 s.

### 2.3.13. Positron annihilation lifetime spectroscopy (PALS)

Disk-shaped samples (diameter 10 mm, thickness = 2 mm) were prepared by pressing the powdered cellulose derivatives. Spectra were acquired on a fast-fast coincidence system (PLS-414 A, EG&G) with a time resolution of = 250 ps. Data were analyzed using the LT-9.0 software package.

### 2.3.14. X-ray photoelectron spectroscopy (XPS)

The samples were irradiated with monochromatic Al K Alpha (100 eV) using a spot size of 500  $\mu\text{m} \times 500 \mu\text{m}$  (ESCALAB 250, USA). In addition, high-resolution scan XPS spectra of Na 1 s and Cl 2p were recorded with a pass energy of 30 eV, and the energy step size was 0.100 eV.

## 3. Results and discussion

### 3.1. Preparation of cellulose ester via alkali cellulose

In this study, we developed a heterogeneous mechanochemical method to synthesize cellulose esters with a high degree of substitution (DS), eliminating the need for conventional acid anhydrides or pyridine. The procedure involves the ball-milling of cellulose with sodium hydroxide solution to generate alkali cellulose, followed by the direct addition of acyl chloride to the same milling pot. After continued grinding, the corresponding cellulose ester was obtained.

Acyl chlorides were chosen over epoxy or halogenated alkanes based on preliminary screening, which confirmed their superior compatibility with the reaction medium (Fig. S1, Supporting Information). Prior to esterification, ball-milling pretreatment effectively reduced the crystallinity of cellulose while preserving its degree of polymerization (Fig. 1b). This mechanical disruption of the native hydrogen-bonding network facilitated the subsequent grafting reaction (Kuga & Wu, 2019; Sergienko et al., 2024). Successful esterification was verified by  $^{13}\text{C}$  NMR spectroscopy, which further revealed the regioselectivity of the

process: acyl chlorides bearing a benzene ring reacted preferentially with the primary hydroxy group at the C-6 position, followed by substitution at the secondary hydroxyls of C-2 and C-3 (Fig. 1c, Fig. S2, Supporting Information).

Compared with cellulose esters prepared by traditional homogeneous methods, the product from this heterogeneous route showed broader peaks in the  $^1\text{H}$  NMR spectrum (Fig. 1d, Fig. S9, Supporting Information), reflecting the inherent substitution heterogeneity typical of solid-state reactions. Nevertheless, the average DS calculated from NMR integrals reached approximately 2.53 (Table S1, Supporting Information), confirming the efficacy of this mechanochemical approach for obtaining highly substituted cellulose esters.

### 3.2. Influence of reagent activity on the reaction process and synthesis of diverse cellulose esters

Acyl chlorides are highly susceptible to hydrolysis in the presence of water, mitigating this hydrolysis was paramount. To address this, we selected acyl chlorides conjugated with  $\pi$  systems (e.g., benzene rings). The conjugation between the aromatic  $\pi$  electrons and the carbonyl  $\pi$  bond reduces the partial positive charge on the carbonyl carbon, thereby lowering its electrophilicity and hydrolysis rate. Furthermore, the inherent hydrophobicity of aromatic structures provides an additional barrier against water, further suppressing hydrolysis (Wang & Ganesan, 2000; Wang & Geroghiou, 2002). (It should be noted that benzyl chloroformate, also included in the initial screening, is a chloroformate ester reagent which exhibits distinct chemistry as it forms carbonate linkages. Its inclusion is justified by its high electrophilicity, which stems from the strong electron-withdrawing inductive effect of the benzyloxy group, making it a relevant point of comparison for general reactivity trends under the mechanochemical conditions.).

To validate this strategy, three conjugated (low-electrophilicity) and three non-conjugated (high-electrophilicity) acyl chlorides were used under identical mechanochemical conditions. The degree of substitution (DS) was evaluated via both FTIR (by integrating the carbonyl absorption area, Fig. 2a and Fig. S2, Supporting Information) and mass-balance calculations (Fig. 2b). Solid-state  $^{13}\text{C}$  NMR spectra of the corresponding esters further corroborated these trends (Fig. S4, Supporting Information). Cellulose esters derived from the high-electrophilicity acyl chlorides exhibited DS values below 0.9, while those from low-electrophilicity, conjugated chlorides consistently yielded DS > 1.5 (Fig. 2b). These complementary results confirm that low-electrophilicity acyl chlorides are significantly more effective for esterification with alkali cellulose in this aqueous-alkaline medium.

Building on this finding, we systematically optimized reaction parameters (alkali type/concentration, molar ratio, milling speed, temperature, and time) using *p*-methylbenzoyl chloride to maximize the DS (Figs. S5-S6, Supporting Information). Notably, lower reaction



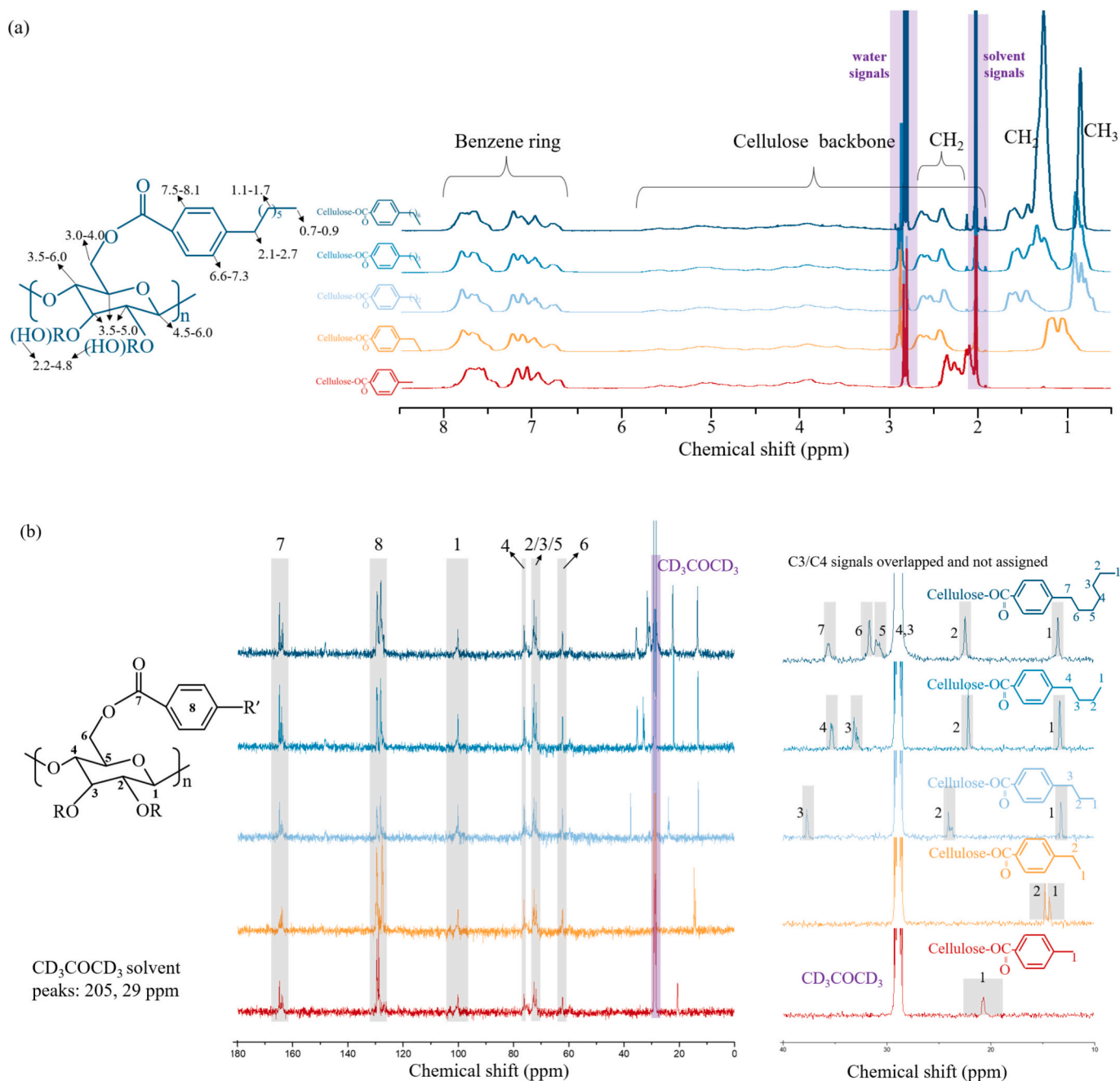


**Fig. 3.**  $^1\text{H}$  NMR (a) and  $^{13}\text{C}$  NMR (b) spectra (in acetone- $d_6$ ) of the synthesized cellulose esters with different para-alkyl substituents (methyl to heptyl).

temperatures were found to be crucial; although elevated temperatures theoretically accelerate the acylation, they disproportionately promote acyl chloride hydrolysis, resulting in a lower net DS—a trend consistent with prior studies (Wang & Ganesan, 2000; Wang & Geroghiou, 2002). Through this optimization, a series of five cellulose esters bearing different para-alkyl substituents (methyl to heptyl) were successfully synthesized with high DS values ( $> 2.5$ , as determined by  $^1\text{H}$  NMR, Table S1–S6, Supporting Information). High-resolution XPS analysis further confirmed that the obtained products were thoroughly purified, showing no detectable signals for sodium or chlorine, which verifies the effective removal of inorganic residues such as NaOH and NaCl (Fig. S7, Supporting Information).

The  $^1\text{H}$  NMR spectra of these five esters are presented in Fig. 3a. The aromatic proton signals (6.5–8.5 ppm) are virtually identical across the series. For the methyl derivative, the deshielding effect of the adjacent

benzene ring shifts the methyl protons upfield ( $>2$  ppm), obscuring the characteristic aliphatic region. As the alkyl chain lengthens, the influence of the benzene ring attenuates, causing the terminal methyl protons to shift downfield; concurrently, the integrated intensity of the methylene signals increases progressively. These spectral trends are in full agreement with the expected structures.

Solution-state  $^{13}\text{C}$  NMR spectra acquired in acetone- $d_6$  further confirmed the molecular structures (Fig. 3b). Although the limited solubility resulted in a higher signal-to-noise ratio compared with conventional small-molecule spectra, all key carbon signals were clearly identifiable. For the longest-chain derivative (heptyl), the C3/C4 signals overlapped with the solvent peak. Overall, the  $^{13}\text{C}$  NMR data are fully consistent with the expected structures of the cellulose esters and corroborate the trends observed in the  $^1\text{H}$  NMR spectra.

Notably, achieving a fully quantitative degree of substitution (DS =

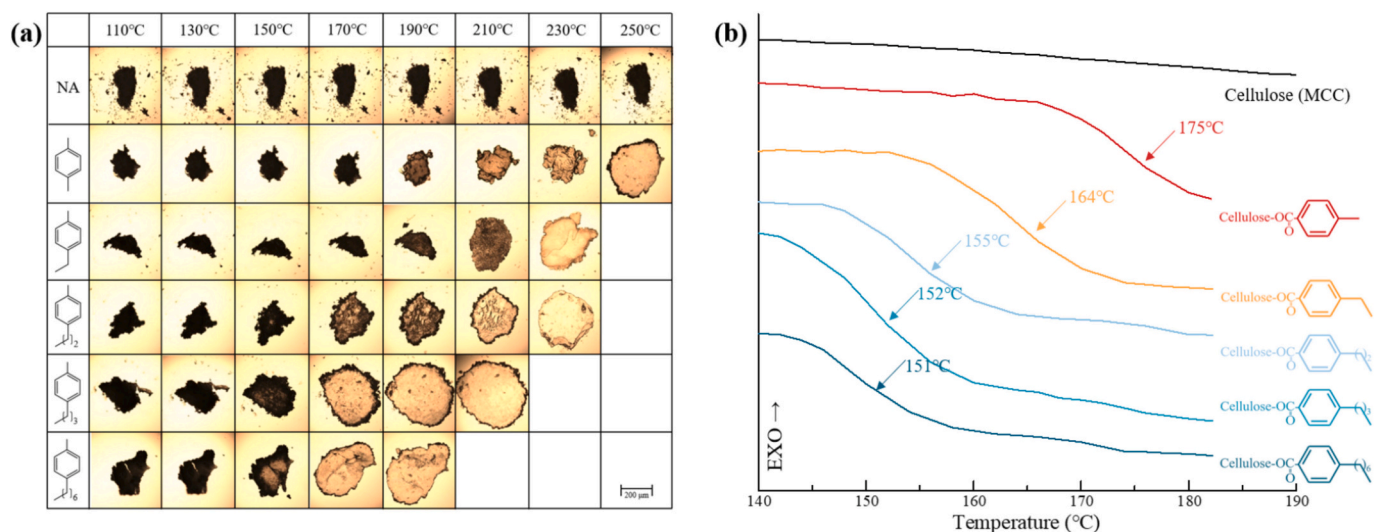


Fig. 4. Thermal behavior of cellulose esters: (a) Polarized optical micrographs showing melting progression upon heating; (b) DSC thermograms.

3.0) in heterogeneous cellulose esterification remains inherently challenging. Several interrelated factors contribute to this limitation (Fox et al., 2011; Kostag et al., 2019; Kwatra et al., 1992): (i) steric hindrance from the introduced substituents, (ii) the reversible nature of the esterification equilibrium, and (iii) trace moisture competing with the desired reaction. Furthermore, cellulose esters with a DS of approximately 2.5 not only reflect the controlled nature of the reaction but are also fully sufficient for thermal processing-industrial cellulose acetate, for instance, typically operates at a DS around 2.5.

In summary, high-DS cellulose esters were successfully synthesized in the presence of water by integrating four key strategies: (a) employing conjugated acyl chlorides to reduce inherent electrophilicity, (b) maintaining a low reaction temperature to suppress hydrolysis, (c) leveraging the hydrophobic character of aromatic reagents to shield the acyl chloride from water, and (d) utilizing ball-milling to mechanically activate cellulose by disrupting its hydrogen-bond network. This combined approach eliminates the need for traditional, toxic mediators such as pyridine or anhydrides, and the lower hydrolysis propensity of the conjugated acyl chlorides themselves enhances the overall safety and industrial potential of the process. Looking forward, the present method is, in principle, extendable to aliphatic acyl chloride systems; however, this will likely require additional process adaptations—such as more rigorous dehydration of the alkali cellulose or the use of co-solvents—to further suppress the rapid hydrolysis of these more sensitive reagents.

### 3.3. Structure-dependent thermal, processing, and mechanical properties of cellulose esters

The thermal, melt-processing, and mechanical properties of the synthesized cellulose esters—each consisting of a rigid benzene ring and a variable aliphatic side chain—were systematically investigated to establish clear structure-property relationships.

#### 3.3.1. Thermal behavior

All five cellulose esters exhibited clear thermal transitions in DSC analysis (Fig. 4b), in contrast to microcrystalline cellulose (MCC), which showed no melting endotherm due to its extensive hydrogen-bond network. Optical microscopy under heating visually confirmed the onset of flow upon melting (Fig. 4a).

The glass-transition temperature ( $T_g$ ) decreased progressively with increasing alkyl-chain length: from 175 °C for the methyl-substituted derivative to 152 °C for the butyl analogue (Fig. 4b). Extending the alkyl chain beyond butyl resulted in only marginal further reduction in  $T_g$ , likely due to enhanced chain entanglement that restricts segmental

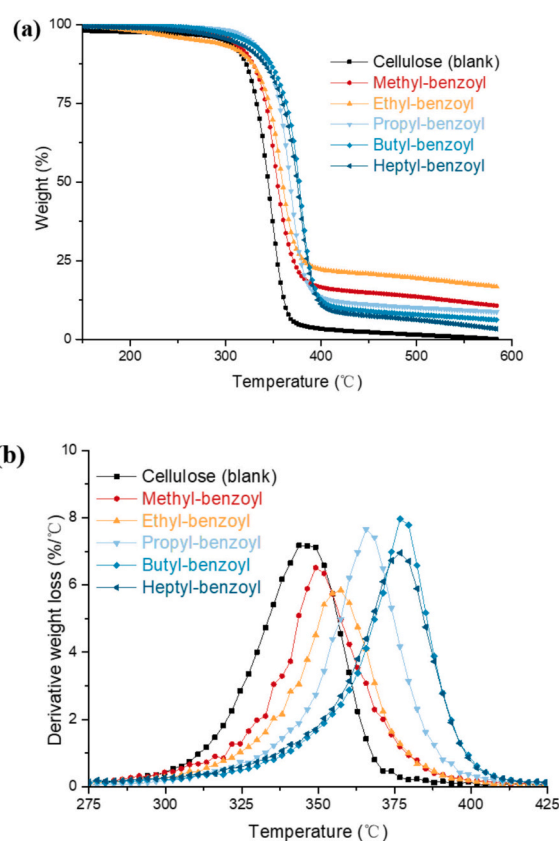


Fig. 5. Thermal stability of cellulose esters: (a) TGA weight-loss curves; (b) Derivative thermogravimetric (DTG) curves.

mobility.

#### 3.3.2. Thermal stability and processing window

Thermogravimetric analysis (Fig. 5) revealed that all esters possessed higher thermal stability than native cellulose, with decomposition temperatures elevated by approximately 30 °C. The activation energy ( $E$ ) of thermal decomposition, determined using a reference method (Xu et al., 2020), systematically decreased with increasing side-chain length (Fig. S8, Supporting Information). Pristine cellulose exhibited the

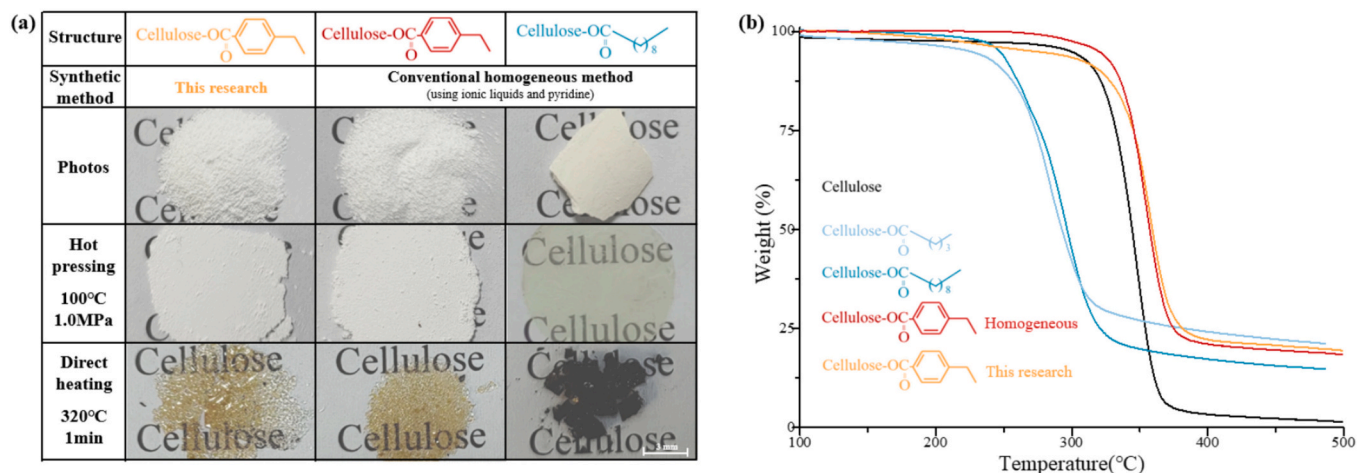


Fig. 6. Melt-processing characteristics versus thermal stability: (a) Schematic comparing the hot-pressing and melt-drawing behavior of different ester types; (b) TGA onset decomposition temperatures.

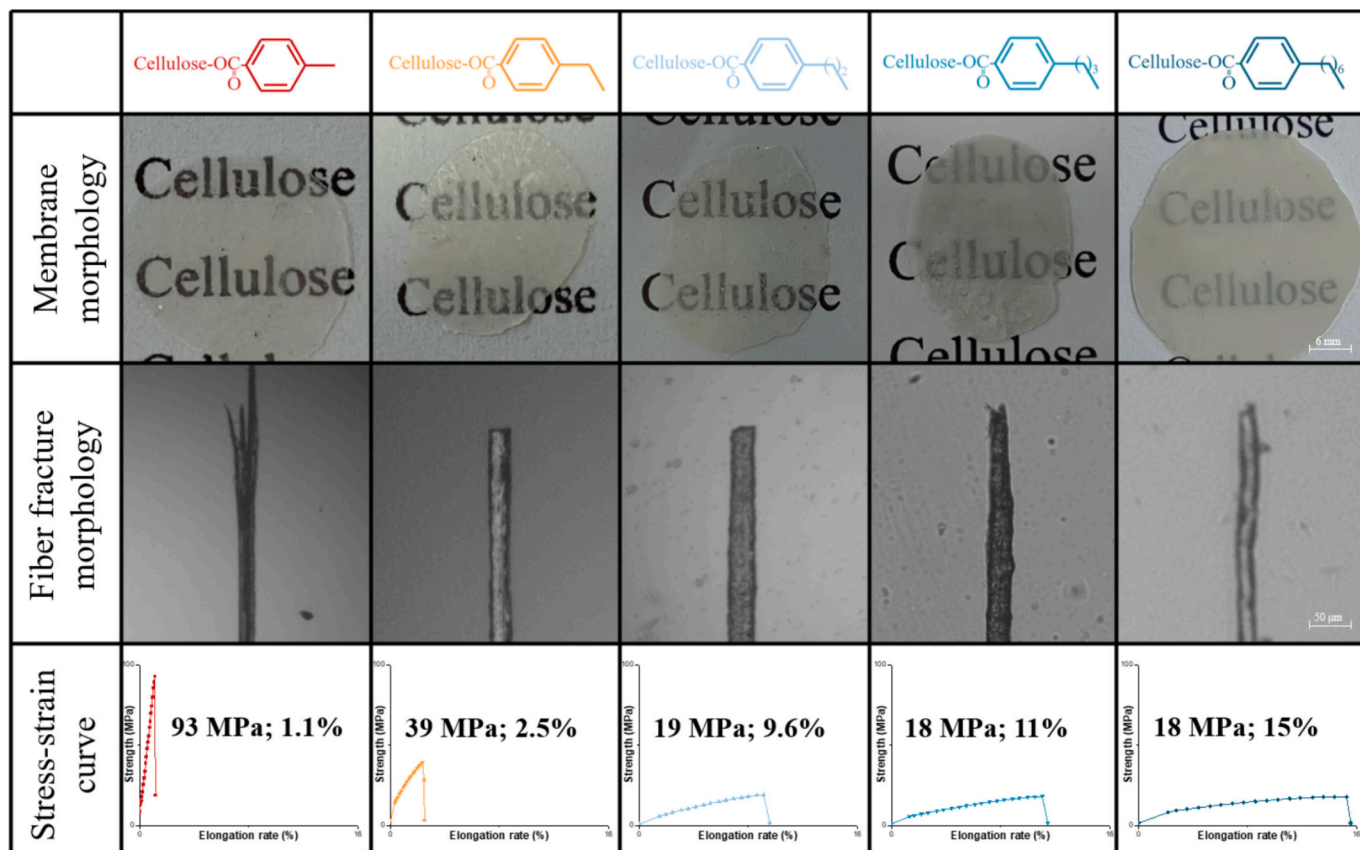


Fig. 7. Comparison of morphology and mechanical properties of different cellulose esters.

highest E value of  $260 \text{ kJ} \cdot \text{mol}^{-1}$ , reflecting its tightly bound crystalline structure. In contrast, the cellulose esters showed progressively lower activation energies: 193 (methyl), 171 (ethyl), 161 (propyl), 127 (butyl), and  $102 \text{ kJ} \cdot \text{mol}^{-1}$  (heptyl). This trend corresponds directly to the disruption of the native hydrogen-bond network and the increase in free volume imparted by the flexible alkyl segments. The combination of a distinct Tg and enhanced-thermal stability establishes an expanded temperature window suitable for melt-based processing.

### 3.3.3. Melt-processing behavior: comparison with conventional esters

The melt-processing behavior of the present benzene-ring-containing

esters was compared with conventional long-chain aliphatic cellulose esters (as evidenced by  $^1\text{H}$  NMR of the long-chain esters, Fig. S9, Supporting Information). The latter show good hot-pressability at moderate temperatures, yet they often degrade before attaining enough melt strength for stable fiber drawing. By contrast, our esters-despite requiring higher softening temperatures-possess both improved thermal stability and sufficient melt cohesion to be drawn continuously into fibers at  $320^\circ\text{C}$  (Fig. 6).

This distinct behavior stems from fundamental structural differences: the rigid benzene ring elevates the decomposition temperature and provides intermolecular associations that preserve melt integrity during



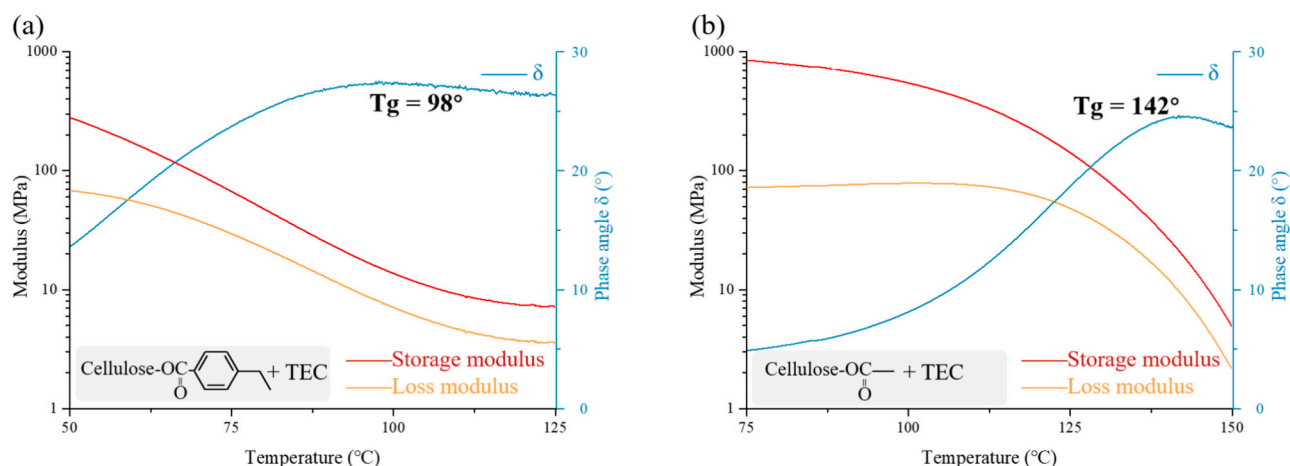


**Fig. 8.** Dynamic mechanical analysis (DMA) of plasticized films: (a) *p*-Ethyl benzoyl cellulose ester with 20% TEC; (b) Commercial cellulose acetate with 20% TEC.

drawing, whereas long aliphatic chains arises mainly from the mobility of the flexible side chains themselves, rather than from the flow of the cellulose backbone. Consequently, while our synthetic route is less suited for preparing long-chain esters (as noted in Section 3.2), this limitation aligns with the material design objective: the benzene-ring-based architecture is intrinsically superior for applications demanding melt-drawing, such as fiber spinning. Moreover, the properties of our heterogeneously synthesized esters match those of analogous materials made by conventional homogeneous methods ( $^1\text{H}$  NMR and  $^{13}\text{C}$  NMR data, Figs. S9, Supporting Information).

### 3.3.4. Mechanical properties of processed films and fibers

In addition, these cellulose esters were hot pressed into a film (180 °C, 5 MPa, 5 min) or pulled into fiber samples (320 °C), and the mechanical properties of the above samples were studied (Fig. 7). Films based on the rigid *p*-methylbenzoyl ester showed high tensile strength (93 MPa) but low elongation at break (1.1%) and failed in a brittle manner. As the alkyl side-chain lengthened, tensile strength gradually decreased while elongation increased significantly, accompanied by a

transition to ductile fracture- a clear manifestation of internal plasticization by the flexible segments. GPC analysis confirmed that the cellulose backbone remained largely intact after the mechanochemical process (Fig. S10, Supporting Information). XRD analysis indicated that although all esters disrupted the native cellulose crystallinity, the more rigid derivatives developed new crystalline reflections (Fig. S11, Supporting Information), which contributed to their higher mechanical strength.

### 3.4. External plasticization and application of cellulose esters

To expand the processing window, we investigated the external plasticization of the cellulose ester (derived from *p*-ethylbenzoyl chloride) using triethyl citrate (TEC), a green plasticizer commonly used in cellulose derivatives. A systematic study of TEC content (0–33 wt%) was conducted. Characterization by optical microscopy, thermogravimetric analysis (TGA), scanning electron microscopy (SEM), X-ray diffraction (XRD), and small-angle X-ray scattering (SAXS) (Fig. S12, Supporting Information) collectively indicated that an appropriate amount of TEC

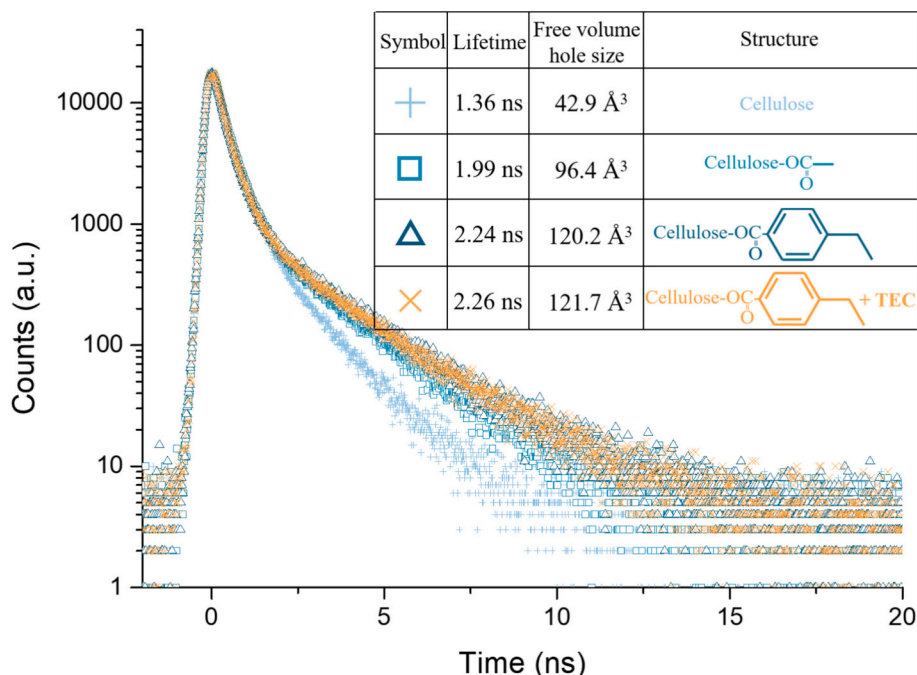


**Fig. 9.** Positron annihilation lifetime spectroscopy (PALS) analysis.



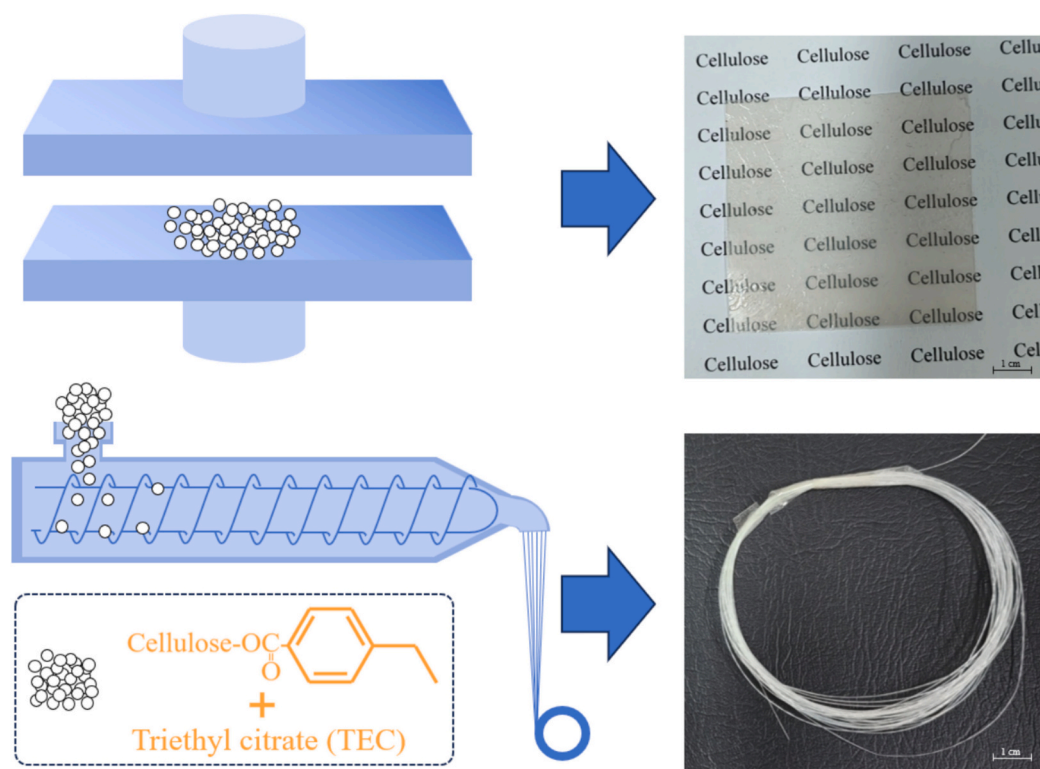


**Fig. 10.** Demonstration of processability: Photographs of continuous fibers and transparent film prepared from plasticized p-ethyl benzoyl cellulose ester (80/20 w/w).

(e.g., 20 wt%) effectively improved processability, while excessive loading led to plasticizer aggregation and phase separation.

Dynamic mechanical analysis (DMA) confirmed that 20 wt% TEC reduced the glass-transition temperature ( $T_g$ ) of our cellulose ester to 98 °C (Fig. 8a). Under identical conditions, commercial cellulose acetate attained a significantly higher  $T_g$  of 142 °C (Fig. 8b; Fig. S13, Supporting Information), highlighting the superior plasticization efficiency of our system.

Notably, positron annihilation lifetime spectroscopy (PALS) revealed that this sharp  $T_g$  drop occurred without a significant increase in free-volume hole size (Fig. 9). This suggests that in the rigid benzene-ring scaffold, TEC primarily acts by shielding strong intermolecular interactions (e.g., hydrogen bonding), rather than by dilating the polymer matrix- a mechanism that preserves melt strength while enabling low-temperature processing.

Consequently, the plasticized cellulose ester (with 20 wt% TEC) exhibited excellent thermal processability, allowing it to be readily fabricated into large, transparent films and continuous fibers via melt-pressing and drawing (Fig. 10), demonstrating its direct potential for practical applications (The mechanical properties are shown in Fig. S14, Supporting Information).

#### 4. Conclusion

In summary, this work presents a one-pot mechanochemical strategy for the synthesis of high-substitution cellulose esters, circumventing the need for traditional toxic reagents such as pyridine or acid anhydrides. The method converts cellulose into alkali cellulose by using aqueous NaOH, followed by ball-milling with benzene-ring-containing acyl chlorides. The conjugated and hydrophobic nature of these reagents, combined with low reaction temperatures, effectively suppressed hydrolysis and enabled efficient esterification, yielding products with a degree of substitution exceeding 2.5.

Through rational molecular design- varying the length of the alkyl

side chain attached to the rigid benzene ring- we achieved precise control over the thermal and mechanical properties of the resulting esters. The introduction of flexible segments reduced the glass-transition temperature, while the aromatic core preserved thermal stability and, critically, provided the melt strength required for demanding processes such as fiber drawing. This combination of rigidity and flexibility distinguishes our materials from conventional long-chain cellulose esters, which lack sufficient melt integrity for spinning.

External plasticization with triethyl citrate further enhanced the processability, lowering the  $T_g$  to 98 °C without altering the fundamental free-volume architecture—a behavior attributed to the shielding of intermolecular interactions rather than matrix dilation. The plasticized esters were readily processed into transparent films and continuous fibers, demonstrating their potential for practical thermal-shaping applications.

Collectively, this study establishes not only a sustainable heterogeneous synthesis route but also a structure-guided design principle for cellulose-based thermoplastics, offering a versatile platform for developing high-performance, processable biomaterials from renewable resources.

#### CRediT authorship contribution statement

**Zhongkai Xu:** Writing – review & editing, Writing – original draft, Visualization, Validation, Supervision, Software, Resources, Project administration, Methodology, Investigation, Funding acquisition, Formal analysis, Data curation, Conceptualization. **Fangyue Cheng:** Methodology, Investigation. **Qingbo Zhao:** Methodology. **Zhenxing Wu:** Methodology. **Peng Wei:** Writing – review & editing. **Chunzu Cheng:** Writing – review & editing. **Shi-Zhong Luo:** Writing – review & editing.

## Consent for publication

All the authors agreed with the addition of authors in this paper; all the authors agreed with the rearrangement of the names.

## Ethical approval

Written informed consent was obtained from all the participants prior to the enrolment (or for the publication) of this study (or case report).

## Funding

Not applicable.

## Declaration of competing interest

The authors declared that they have no conflicts of interest to this work.

## Acknowledgments

The authors wish to express deepest thanks and appreciation for China Textile Academy, for the facilities provided. The authors would like to acknowledge the support from the QiHuang Yingcai Program of Beijing University of Chinese Medicine.

## Appendix A. Supplementary data

Supplementary data to this article can be found online at <https://doi.org/10.1016/j.carbpol.2026.125258>.

## Data availability

The authors do not have permission to share data.

## References

- Ahokas, P., Kunnari, V., Majoinen, J., Harlin, A., & Mäkelä, M. (2025). Plasticizer mixing improved regenerated cellulose films as an alternative to plastics. *ACS Sustainable Chemistry & Engineering*, 13, 10771–10779.
- Bonifacio, A., Bonetti, L., Piantanida, E., & Nardo, L. D. (2023). Plasticizer design strategies enabling advanced applications of cellulose acetate. *European Polymer Journal*, 197, Article 112360.
- Bussiere, P. O., Gardette, J. L., & Therisa, S. (2014). Photodegradation of celluloid used in museum artifacts. *Polymer Degradation and Stability*, 107, 246–254.
- Chatel, G., & Varma, R. S. (2019). Ultrasound and microwave irradiation: Contributions of alternative physicochemical activation methods to Green Chemistry. *Green Chemistry*, 21, 6043–6050.
- Chen, Z., Zhang, J., Xiao, P., Tian, W., & Zhang, J. (2018). Novel thermoplastic cellulose esters containing bulky moieties and soft segments. *ACS Sustainable Chem. Eng.*, 6, 4931–4939.
- Fox, S., Li, B., Xu, D., & Edgar, K. (2011). Regioselective Esterification and Etherification of Cellulose: A Review. *Biomacromolecules*, 12, 1956–1972.
- Ge, W., Shuai, J., Wang, Y., Zhou, Y., & Wang, X. (2022). Progress on chemical modification of cellulose in “green” solvents. *Polymer Chemistry*, 13, 359.
- Hirose, D., Kusuma, S. B. W., Ina, D., Wada, N., & Takahashi, K. (2019). Direct one-step synthesis of a formally fully biobased polymer from cellulose and cinnamon flavor. *Green Chemistry*, 21, 4927–4931.
- Hou, D., Li, M., Li, P., Zhou, L., Zhang, K., Liu, Z., Yang, W., & Yang, M. (2023). Efficient Conversion of Cellulose to Thermoplastics by Mechanochemical Esterification. *ACS Sustainable Chemistry & Engineering*, 11, 7655–7663.
- Hou, D., Li, M., Yan, C., Zhou, L., Liu, Z., Yang, W., & Yang, M. (2021). Mechanochemical preparation of thermoplastic cellulose oleate by ball milling. *Green Chemistry*, 23, 2069–2078.
- Hou, D., Li, P., Zhang, K., Li, M., Feng, Z., Yan, C., Liu, C., & Yang, M. (2024). Insight into the Feasibility of Fatty Acyl Chlorides with 10-18 Carbons for the Ball-Milling Synthesis of Thermoplastic Cellulose Esters. *Biomacromolecules*, 25, 1923–1932.
- Hou, D., Yuan, P., Feng, Z., An, M., Li, P., Liu, C., & Yang, M. (2023). Sustainable conversion regenerated cellulose into cellulose oleate by sonochemistry. *Frontiers of Chemical Science and Engineering*, 17, 1096–1108.
- Huang, Z., Tan, Y., Zhang, Y., Liu, X., Hu, H., Qin, Y., & Huang, H. (2012). Direct production of cellulose laurate by mechanical activation-strengthened solid phase synthesis. *Bioresource Technology*, 118, 624–627.
- Jiang, X., Bai, Y., Chen, X., & Liu, W. (2020). A review on raw materials, commercial production and properties of lyocell fiber. *Journal of Bioresources and Bioproducts*, 5, 16–25.
- Joshi, G., Rana, V., Naithani, S., Varshney, V., Sharma, A., & Rawat, J. (2019a). Chemical modification of waste paper: An optimization towards hydroxypropyl cellulose synthesis. *Carbohydrate Polymers*, 223, Article 115082.
- Joshi, G., Rana, V., Naithani, S., Varshney, V., Sharma, A., & Rawat, J. (2019b). Chemical modification of waste paper: An optimization towards hydroxypropyl cellulose synthesis. *Carbohydrate Polymers*, 223, Article 115082.
- Kita, G., Mazume, T., Nakashima, T., & Sakurada, I. (1926). Ueber die Veresterung der Alkalicellulose I. *Memoirs of the College of Engineering, Kyoto Imperial University.*, 4, 129–145.
- Klemm, D., Philipp, B., Heinze, T., Heinze, U., & Wagenknecht, W. (1998). *Comprehensive cellulose chemistry. Volume 2: Functionalization of cellulose*.
- Kostag, M., Gericke, M., Heinze, T., & Seoud, O. (2019). Twenty-five years of cellulose chemistry: innovations in the dissolution of the biopolymer and its transformation into esters and ethers. *Cellulose*, 26, 139–184.
- Kuga, S., & Wu, M. (2019). Mechanochemistry of cellulose. *Cellulose*, 26, 215–225.
- Kwatra, H., Caruthers, J., & Tao, B. (1992). Synthesis of long chain fatty acids esterified onto cellulose via the vacuum-acid chloride process. *Industrial and Engineering Chemistry Research*, 31, 2647–2651.
- Lease, J., Kawano, T., & Andou, Y. (2021). Esterification of Cellulose with Long Fatty Acid Chain through Mechanochemical Method. *Polymers*, 13, 4397.
- Li, C., Wu, J., Shi, H., Xia, Z., Sahoo, J. K., Yeo, J., & Kaplan, D. L. (2022). Fiber-based biopolymer processing as a route toward sustainability. *Advanced Materials*, 34, Article 2105196.
- Li, C., Zhang, X., Chen, H., Wang, H., Huang, J., Li, T., ... Dong, W. (2025). Thermoformed, thermostable, waterproof and mechanically robust cellulose-based bioplastics enabled by dynamically reversible thia-Michael reaction. *International Journal of Biological Macromolecules*, 295, Article 139567.
- Li, J., Zhang, H., Scarpante, G. G., Lawton, D. J. W., Marway, H. S., & Thompson, M. R. (2020). Solvent-free modification of lignocellulosic wood pulp into a melt-flowable thermoplastic. *Cellulose*, 28, 1055–1069.
- Li, M., Hou, D., Li, P., Feng, Z., Huang, Y., Wang, F., Zhai, Y., Sun, X., Zhang, K., Yin, B., Yang, W., & Yang, M. (2024). One-Step Solvent-Free Strategy to Efficiently Synthesize High-Substitution Cellulose Esters. *ACS Sustainable Chemistry & Engineering*, 12, 9669–9681.
- Li, M., Sun, S., Xu, F., & Sun, R. (2011). Cold NaOH/urea aqueous dissolved cellulose for benzylation: Synthesis and characterization. *European Polymer Journal*, 47, 1817–1826.
- Li, T., Chen, C., Brozena, A. H., Zhu, A. Y., Xu, L., Driemeier, C., ... Hu, L. (2021). Developing fibrillated cellulose as a sustainable technological material. *Nature*, 590, 47–56.
- Li, X., Qiu, X., Yang, X., Zhou, P., Guo, Q., & Zhang, X. (2024). Multi-Modal Melt-Processing of Birefringent Cellulosic Materials for Eco-Friendly Anti-Counterfeiting. *Advanced Materials*, 36, 2407170.
- Lu, Z., Xing, Y., Zheng, W., Han, Y., Zhang, Z., Wang, J., & Liu, C. (2025). Hydrogen-Bonding Cross-Linking Agent-Reinforced Chitosan/Cellulose Composite Films for Fresh Fruit Preservation: An Experimental and Theoretical Study. *ACS Sustainable Chemistry & Engineering*, 13, 10597–10610.
- Mendes, I. F., Prates, A., & Evtuguin, D. V. (2021). Production of rayon fibres from cellulosic pulps: State of the art and current developments. *Carbohydrate Polymers*, 273, Article 118466.
- Mori, R. (2023). Replacing all petroleum-based chemical products with natural biomass-based chemical products: a tutorial review. *RSC Sustainability*, 1, 179–212.
- Mphateng, T. N., Mapossa, A. B., Mokheba, T., Ray, S. S., & Sundararaj, U. (2025). Melt processing of cellulose acetate for controlled release applications - A review. *Macromolecular Materials and Engineering*, 310, Article e00117.
- Naser, A. Z., Deiab, I., & Darras, B. M. (2021). Poly(lactic acid) (PLA) and poly(hydroxyalkanoates) (PHAs), green alternatives to petroleum-based plastics: A review. *RSC Advances*, 11, 17151–17196.
- Nemr, A. E., Ragab, S., & Sikaily, A. E. (2016). Testing zinc chloride as a new catalyst for direct synthesis of cellulose di- and tri-acetate in a solvent free system under microwave irradiation. *Carbohydrate Polymers*, 151, 1058–1067.
- Pan, H., Tong, M., Wang, X., Huang, B., Yu, X., Zhang, C., & Wang, Y. (2024). Fully Biobased High-Strength and High-Toughness Double Cross-Linked Cellulose Hydrogel for Flexible Electrolytes. *ACS Sustainable Chemistry & Engineering*, 12, 18231–18244.
- Pei, M., Peng, X., Shen, Y., Yang, Y., Guo, Y., Zheng, Q., ... Sun, H. (2020). Synthesis of water-soluble, fully biobased cellulose levulinate esters through the reaction of cellulose and alpha-algelica lactone in a DBU/CO<sub>2</sub>/DMSO solvent system. *Green Chemistry*, 22, 707–717.
- Qian, T., Qin, C., Zhang, J., Shi, B., Wei, Y., Wang, C., ... Liu, Y. (2025). Sustainable, biodegradable, and recyclable bioplastics derived from renewable carboxymethyl cellulose and waste walnut shell. *International Journal of Biological Macromolecules*, 299, Article 140130.
- Sawatdee, S., Botalo, A., Pongchaikul, P., Posoknistakul, P., Phadungbut, P., Intra, P., ... Sakdaronnarong, C. (2025). Design of Multilayer Cellulose-Based Filters Combined with Zeolitic Imidazole Framework and Silica Nanoparticles for Particulate Matter Filtration and Antibacterial Properties. *ACS Sustainable Chemistry & Engineering*, 13, 7074–7087.
- Sergienko, J. P., Sillard, C., Belgacem, M. N., & Bras, J. (2024). Simultaneous Comminution and Hydrophobization of Cellulose Fibers by Mechanochemistry. *ACS Sustainable Chemistry & Engineering*, 12, 16540–16552.

- Sessini, V., Haseeb, B., Boldiza, A., & Re, G. L. (2021). Sustainable pathway towards large scale melt processing of the new generation of renewable cellulose-polyamide composites. *RSC Advances*, 11, 637–656.
- Shojaeiarani, J., Bajwa, D. S., & Stark, N. M. (2018). Green esterification: A new approach to improve thermal and mechanical properties of poly(lactic acid) composites reinforced by cellulose nanocrystals. *Journal of Applied Polymer Science*, 135, 46468.
- Siepmann, J., & Peppas, N. (2012). Modeling of drug release from delivery systems based on hydroxypropyl methylcellulose (HPMC). *Advanced Drug Delivery Reviews*, 64, 163–174.
- Song, J., Chen, C., Zhu, S., Zhu, M., Dai, J., Ray, U., ... Hu, L. (2018). Processing bulk natural wood into a high-performance structural material. *Nature*, 554, 224–228.
- Sundman, O., Gillgren, T., & Broström, M. (2015). Homogenous benzylation of cellulose - impact of different methods on product properties. *Cellulose Chemistry and Technology*, 49, 745–755.
- Tanaka, S., Iwata, T., & Iji, M. (2016). Solvent effects on heterogeneous synthesis of cardanol-bonded cellulose thermoplastics. *Polymer*, 99, 307–314.
- Tanaka, S., Iwata, T., & Iji, M. (2017). Long/Short Chain Mixed Cellulose Esters: Effects of Long Acyl Chain Structures on Mechanical and Thermal Properties. *ACS Sustainable Chemistry & Engineering*, 5(2), 1485–1493.
- Thiebaud, S., & Borredon, M. E. (1995). Solvent-free wood esterification with fatty acid chlorides. *Bioresour Technol.*, 52, 169–173.
- Toyama, K., Soyama, M., Tanaka, S., & Iji, M. (2015). Development of cardanol-bonded cellulose thermoplastics: high productivity achieved in two-step heterogeneous process. *Cellulose*, 22, 1625–1639.
- Wang, H., & Ganesan, A. (2000). Total Synthesis of the Fumiquinazoline Alkaloids: Solution-Phase Studies. *The Journal of Organic Chemistry*, 65, 1022–1030.
- Wang, J., Liang, Y., Chen, Y., Wan, H., Jin, W., Luo, T., Chen, Y., Wei, P., Huang, S., He, Y., Wang, Y., & Xia, Y. (2025). Highly degradable bio-based plastic with water-assisted shaping process and exceptional mechanical properties. *Carbohydrate Polymers*, 347, Article 122773.
- Wang, L., Gardner, D. J., Wang, J., Yang, Y., Tekinalp, H. L., Tajvidi, M., ... Anderson, J. (2020). Towards industrial-scale production of cellulose nanocomposites using melt processing: A critical review on structure-processing-property relationships. *Compos. Part B-Eng.*, 201, Article 108297.
- Wang, Y., & Geroghiou, P. E. (2002). First enantioselective total synthesis of (–)-Tejedine. *Organic Letters*, 4, 2675–2678.
- Xia, Z., Lu, H., Xia, G., Zhang, J., Zhou, Y., Mi, Q., Li, J., & Zhang, J. (2023). Tough and Strong All-Biomass Plastics from Agricultural and Forest Wastes via Constructing an Aggregate of Hydrogen-Bonding Networks. *ACS Sustainable Chemistry & Engineering*, 11, 9153–9162.
- Xu, F., Zhang, X., Zhang, F., Jiang, L., Zhao, Z., & Li, H. (2020). TG-FTIR for kinetic evaluation and evolved gas analysis of cellulose with different structures. *Fuel*, 268, Article 117365.
- Xu, R., Yin, C., You, J., Zhang, J., Mi, Q., Wu, J., & Zhang, J. (2024). Sustainable, thermoplastic and hydrophobic coating from natural cellulose and cinnamon to fabricate eco-friendly catering packaging. *Green Energy & Environment*, 9, 927–936.
- Yin, C., An, H., Wu, Q., Wang, X., Wang, J., Liao, X., ... Zhang, J. (2026). Bulky rigid substituent to enhance the chain mobility of cellulose for bio-degradable thermoplastics. *Advanced Functional Materials*, 36, Article e10529.
- Yin, C., Wang, Y., Wang, J., You, Y., Wang, X., Zhang, J., & Zhang, J. (2024). Aquathermoplastics: Recycling plastics with water. *Advanced Functional Materials*, 35, 2417119.
- Yun, C., Liu, C., Zhao, G., Chen, C., Jia, Y., Zhou, Y., ... Yang, W. (2025). Anhydride-form cellulose derivatives: Synthesis, in situ reactive separation, and solvent recycling. *Angewandte Chemie, International Edition*, 64, Article e202514191.
- Zhang, S., Chen, C., Duan, C., Hu, H., Li, H., Li, J., Liu, Y., Ma, X., Stavik, J., & Ni, Y. (2018). Regenerated Cellulose by the Lyocell Process, a Brief Review of the Process and Properties. *BioResources*, 13, 4577–4592.
- Zhong, X., Tong, X., Yu, M., Li, H., Li, H., Li, X., Gibril, M., Zhang, Y., & Han, K. (2013). Graft Polymerization of L-Lactide onto Cellulose in IONIC LIQUID via Twin Screw Extruder. *Advanced Materials Research*, 658, 8–12.
- Zhou, J., You, M., Xu, J., Jin, Y., Li, D., Xu, Z., & Chen, C. (2024). All-Cellulose Bioplastics from Waste Wood Particles. *ACS Sustainable Chemistry & Engineering*, 12, 9550–9557.
- Zhu, E., Xu, G., Ye, X., Yang, J., Yang, H., Wang, D., Shi, Z., & Deng, J. (2021). Preparation and characterization of hydrothermally pretreated bamboo powder with improved thermoplasticity by propargyl bromide modification in a heterogeneous system. *Adv. Compos. Hybrid Ma.*, 4, 1059–1069.